# Evidence for the Prion Hypothesis: Induction of the Yeast [PSI<sup>+</sup>] Factor by in VitroConverted Sup35 Protein

Helmut E. Sparrer,<sup>1</sup> Alex Santoso,<sup>1</sup> Francis C. Szoka Jr.,<sup>2</sup> Jonathan S. Weissman<sup>1\*</sup>

Starting with purified, bacterially produced protein, we have created a [PSI<sup>+</sup>]-inducing agent based on an altered (prion) conformation of the yeast Sup35 protein. After converting Sup35p to its prion conformation in vitro, we introduced it into the cytoplasm of living yeast using a liposome transformation protocol. Introduction of substoichiometric quantities of converted Sup35p greatly increased the rate of appearance of the well-characterized epigenetic factor [PSI<sup>+</sup>], which results from self-propagating aggregates of cellular Sup35p. Thus, as predicted by the prion hypothesis, proteins can act as infectious agents by causing self-propagating conformational changes.

Prions are infectious agents that lack nucleic acid and are composed of an altered, B sheetrich conformation of a normal cellular protein (1). Prion infectivity is thought to result from the ability of the prion protein in its altered conformation to bind to the normal form of the protein and catalyze its conversion to the infectious conformation. While originally identified as the causative agent for a set of related transmissible spongiform encephalopathies (TSEs), including Creutzfeld-Jacob disease in humans, scrapie in sheep, and mad cow disease in cattle, self-propagating β sheet-rich protein aggregates also underlie a variety of noninfectious neurodegenerative diseases (2). These include the relatively common disorders Alzheimer's disease and Parkinson's disease, as well as dominantly inherited polyglutamine repeat disorders, such as Huntington's disease (3-5). In addition to the role in human pathogenesis, B sheet-rich aggregates of glutamine and asparagine-rich domains mediate inheritance of the non-Mendelian, prionlike traits [PSI+] and [URE3] in Saccharomyces cerevisiae (6, 7).

The facile genetics of *S. cerevisiae* has made the yeast prions a rich source of information on the mechanism of prion propagation in vivo as well as the role of prion-based inheritance in the normal physiology of a cell. In the case of [*PSI*<sup>+</sup>], the prion protein is a translation termination factor Sup35p (8). Self-replicating aggregates of Sup35p lead to depletion of the cellular pool of the termina-

tion factor, resulting in an enhanced tendency for ribosomes to read through nonsense mutations (9). A modular  $NH_2$ -terminal prion domain of Sup35p is necessary and sufficient for propagation of  $[PSI^+]$  (I0-I3). Sup35p prion function is strongly conserved, but as with mammalian prions, a species barrier inhibits cross-species prion induction (I4-I6). Finally, a major advantage of the [PSI] system is that it is possible to propagate Sup35p aggregates in vitro by using pure proteins (I7-I9).

Although a large body of data demonstrates the central role of self-propagating conformational changes in the above phenomena, in no case to date has the core prediction of the prion hypothesis been demonstrated by creating new infectious material from pure protein in vitro [for recent progress, see (20-22)]. Indeed, despite the success in eliminating nucleic acids from the infectious agents responsible for TSEs, the low infectivity of isolated material [typically there are 100,000 prion protein (PrP) molecules per infectious unit] makes it difficult to rule out a requirement for other nonproteinaceous components (23). Here, we have developed a liposome transformation protocol to test if pure in vitro-converted Sup35p can induce [PSI<sup>+</sup>].

A liposome-based strategy for introducing converted protein into yeast cytoplasm. Efforts to demonstrate prion-based infection by using pure in vitro–converted Sup35p to induce the  $[PSI^+]$  state face two compounding challenges. First, conversion is likely to require introduction of a substantial bolus of highly aggregated protein into the yeast cytoplasm, because effective initiation of Sup35p polymerization in vitro requires addition of  $\sim 0.5\%$  preformed fiber (19). Sec-

ond, cells receiving converted Sup35p have to be identified and selected against the large bulk of cells receiving no protein in order to minimize any contribution from the small ( $\sim 1 \times 10^{-6}$ ), but significant, spontaneous conversion to [PSI+] (7). To overcome these difficulties, we developed a liposome transformation strategy that allowed the simultaneous delivery of both a URA3-marked plasmid and a large bolus of Sup35p aggregates into yeast spheroplasts (Fig. 1). By selecting for growth on media lacking uracil, we could eliminate cells that had not undergone successful fusion.

We first optimized our transformation protocol by monitoring liposome-mediated delivery of the URA3 marked plasmid (24). For preparation of liposomes and encapsulation of macromolecules, we used the reverse-phase evaporation method, which yields large  $(400 \pm 50 \text{ nm})$  liposomes, allowing delivery of volumes approaching 1% of the yeast cytoplasm. To enhance transformation efficiency, we attached liposomes to the surface of

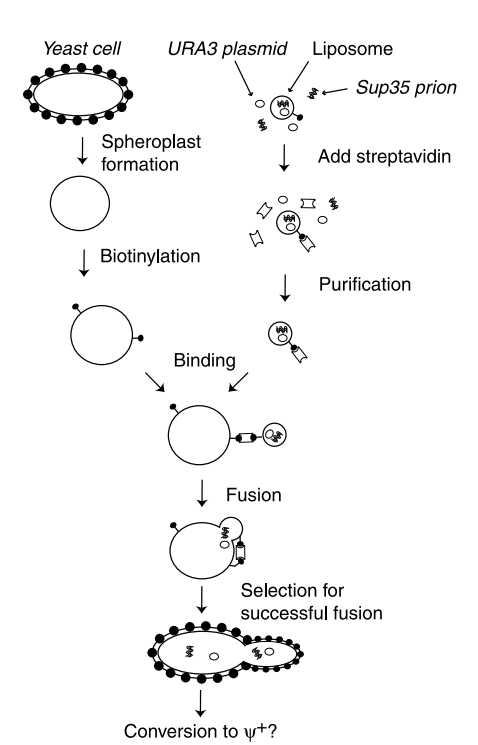


Fig. 1. Schematic representation of the liposome transformation strategy (24, 40). URA3 plasmid (O) and Sup35 NM-His $_7$  ( $\approx$ ) are coencapsulated in biotin-containing liposomes. After purification on a Ficoll density gradient to remove unencapsulated material, the liposomes are bound to the surface of biotinylated yeast spheroplasts, and fusion is induced by the addition of PEG. Surface binding of liposomes to spheroplasts before fusion increases transformation efficiency by two orders of magnitude (24). Cells that undergo successful fusion are selected by growth on medium lacking uracil. Finally, these liposome transformants are examined for conversion to [PSI+].

<sup>&</sup>lt;sup>1</sup>Department of Cellular and Molecular Pharmacology and <sup>2</sup>Department of Pharmaceutical Chemistry, University of California, San Francisco, San Francisco, CA 94143–0450. USA.

<sup>\*</sup>To whom correspondence should be addressed. E-mail: jsw1@itsa.ucsf.edu

yeast spheroplasts by a biotin-streptavidin linkage (Fig. 1) and then induced fusion with polyethylene glycol (PEG). The DNA plasmid delivered by liposome transformation was resistant to deoxyribonuclease I treatment, and efficient transformation required biotin, confirming that the transformation occurred by fusion-mediated delivery of liposome-encapsulated material (24).

Liposome transformation allows introduction of converted Sup35p into yeast. We next used our liposome protocol to introduce converted Sup35 protein into yeast cells. For our conversion experiments, we used a Sup35p fragment (Sup35 NM-His<sub>7</sub>) composed of the glutamine and asparaginerich NH2-terminal domain (N), which plays a critical role in the prion propagation (10–13), and the highly charged middle region (M) followed by a COOH-terminal seven-histidine tag. The protein contained no impurities detectable by SDS-polyacrylamide gel electrophoresis (PAGE) or mass spectrometry and, with the exception of removal of the NH<sub>2</sub>-terminal methionine, the Sup35 NM-His, contained no covalent modifications (expected mass = 29345.1 Daltons, measured mass = 29344.3 Daltons) (24).

By fluorescently labeling Sup35 NM-His<sub>7</sub>, we could directly visualize the different steps of the transformation process. A single cysteine was added to the COOH-terminus of Sup35 NM-His<sub>7</sub> protein, allowing it to be modified with a fluorescein-derived fluorophore ALEXA 488 (24). Before PEG treatment, microscopy revealed fluorescent liposome-encapsulated protein bound to the spheroplast surface in a small fraction (~1 in 50) of cells (Fig. 2A). After PEG treatment, we did not observe liposomes attached to the outside of cells. Rather, a fraction of cells appeared to contain fluorescent material within the cytoplasm, suggesting that the pro-

tein had been delivered to the cell interior (Fig. 2B).

Using Alexa 488–labeled Sup35 NM-His<sub>7</sub> and fluorescence microscopy, we estimated the number of intact liposomes containing encapsulated protein in the liposome preparations. Western blot analysis comparing the amount of Sup35p in a specified number of yeast cells with a 5- or 25-fold larger number of liposomes revealed that a single liposome delivers at most 10% of Sup35 NM-His<sub>7</sub> compared with endogenous full-length Sup35p (Fig. 2C), whereas estimates of cellular Sup35p concentrations indicate that an average liposome delivers at least 2% of endogenous protein (25).

Using a well-characterized in vitro conversion assay (18, 19), we directly demonstrated that the encapsulated protein had formed a state capable of initiating the polymerization of monomeric Sup35 NM-His<sub>7</sub>. After dilution from urea, Sup35 NM-Hisundergoes amyloid fibril formation, which is preceded by a lag phase (~60 min under the present conditions) that is shortened by the addition of catalytic amounts of preformed fibers. After releasing encapsulated protein by cycles of freeze-thawing (Fig. 3) or ether extraction (26), addition of 0.6% of liposome-derived Sup35p NM-His, substantially accelerated the polymerization, whereas addition of an equivalent amount of protein encapsulated in liposomes did not affect conversion.

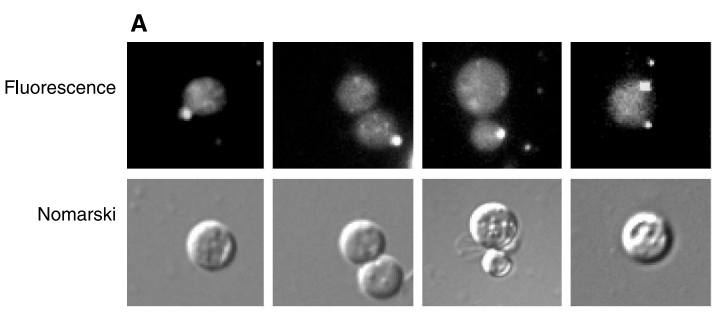
Introduction of Sup35p induces conversion to the  $[PSI^+]$  state. The liposome transformation protocol allowed us to determine if introduction of Sup35 NM-His7 aggregates could initiate the conversion of the cellular pool of Sup35p, resulting in de novo induction of  $[PSI^+]$ . To detect the presence of the  $[PSI^+]$  factor, we used the yeast strain 74D-694 harboring a suppressible nonsense (stop-

codon) mutation in the *ade1* gene (27). In [*psi*<sup>-</sup>] yeast, only truncated, nonfunctional Ade1p is produced, resulting in no growth on media lacking adenine and the accumulation of a red metabolic intermediate on media containing low adenine. By contrast, the [*PSI*<sup>+</sup>] factor causes a nonsense suppression phenotype and production of full-length Ade1p, resulting in growth on media lacking adenine and white-pink colonies on low-adenine media.

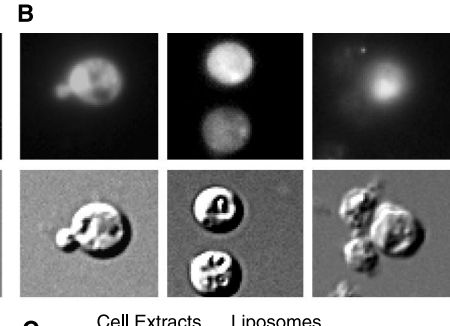
We used this color assay and the adenine prototrophy to screen liposome transformants for putative  $[PSI^+]$  convertants (24). After transformation with liposomes, yeast were plated on media lacking uracil and containing a low-adenine concentration (SD-URA/low ADE), thus selecting for the URA3 plasmid and testing the  $[PSI^+]$  phenotype. We then retested putative [PSI+] colonies for growth on media lacking adenine. Finally, we distinguished true [PSI+] convertants from ADE1 suppressor mutations by growth on media containing low concentrations of guanidine hydrochloride (5 mM), which causes efficient  $[PSI^+]$  curing (28). To ensure that the growth on low-adenine medium did not induce  $[PSI^+]$  formation, we repeated the conversion experiments, plating first on SD-URA media that was rich in adenine. In this case, we examined every liposome transformant for the presence of  $[PSI^+]$ .

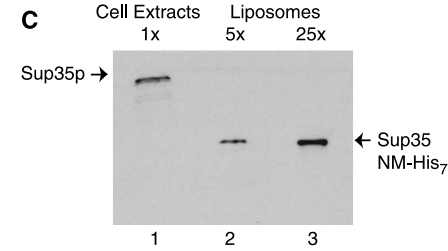
Using Sup35 NM-His<sub>7</sub> at a concentration of 200 µg/ml, we obtained a total of 33 [PSI<sup>+</sup>] colonies from 2214 liposome transformants (Table 1) (29). Increasing the Sup35p concentration in the liposomes to 300 µg/ml substantially decreased the number of URA3 plasmid transformants but did not change the efficiency of [PSI<sup>+</sup>] conversion among these transformants (5 of 287). By contrast, as might be expected from protein-mediated infectivity, when we used a lower

Fig. 2. Visualization of liposome transformation with fluorescently labeled protein. (A) Visualization of liposomes containing fluorescently labeled Sup35 NM-His<sub>7</sub> bound to yeast spheroplasts before PEG-induced fusion (top panels). A single bound liposome is ob-



served in about 1 out of 50 cells (first three panels). Even more rarely, spheroplasts with two or more liposomes are observed (left panel). Also shown are Nomarski images of the same cells (lower panel). (B) Visualization of spheroplasts after PEG-induced fusion. (C) Western blot analysis comparing levels of Sup35p present in cell extracts with Sup35 NM-His $_7$  in a 5- or 25-fold larger number of liposomes. Fluorescent liposomes were quantified by counting in a hematocytometer and related to the amount of yeast cells. Shown is a 5× (lane 2) and 25× (lane 3) excess of liposomes compared with 1× yeast cells expressing endogenous full-length Sup35p (lane 1).





Sup35p concentration (100  $\mu$ g/ml), the efficiency of conversion appeared to decrease (2 of 585).

In a series of assays we confirmed that the converted colonies carried the [PSI<sup>+</sup>] factor. First, even after repeated passages on nonselective media, converted yeast retained the ability to grow on media lacking adenine and formed white-pink colonies on low-adenine media (Fig. 4A). Second, growth on media containing low concentrations of guanidine caused efficient [PSI+] curing, resulting in adenine auxotrophy and reversion to red color (Fig. 4A). Finally, using a previously described centrifugation assay (11, 12), we demonstrated directly that the nonsense readthrough phenotype resulted from aggregation of the cellular Sup35 protein. In [PSI+] convertants, Sup35p fractionated exclusively to the pellet after high-speed centrifugation. By contrast, before conversion or after curing of converted yeast by growth on guanidine-containing media, Sup35p remained largely in the supernatant (Fig. 4B).

A set of further control experiments demonstrated that induction of  $[PSI^+]$  was a specific consequence of introduction of the Sup35p and not simply a by-product of the liposome transformation procedure (Table 1). We repeated the above transformation experiments using liposomes containing only the URA3 plasmid. Out of the 5692 colonies examined, we found only one  $[PSI^+]$  convertant. Similarly, when we incorporated bovine serum albumin (200  $\mu g/ml$ ), a protein that is not associated with prion formation or the  $[PSI^+]$  state, we did

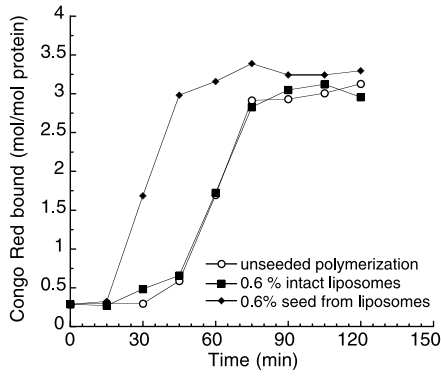


Fig. 3. Liposome-encapsulated Sup35 NM-His $_7$  catalyzes polymerization in vitro. To initiate conversion, concentrated Sup35 NM-His $_7$  was diluted from denaturant to a final concentration of 2.5  $\mu$ M (19). Conversion was allowed to proceed in the absence of added material or in the presence of 0.6% Sup35 NM-His $_7$  either in intact liposomes or released from liposomes by freeze-thawing. At the indicated times, the extent of fibril formation was assayed by addition of the dye Congo red, which specifically binds to amyloid fibers. A similar degree of acceleration was observed when the protein was released from the liposomes by ether extraction (24).

not obtain any convertants among the 2128 colonies examined.

A species barrier in liposome infectivity. A hallmark of prion infection is the existence of species barriers requiring that the amino acid sequence of the infecting protein closely match that of the infected organism (1, 14-16). To test whether similar specificity exists for the liposome transformation, we examined the ability of two Sup35p variants to induce [PSI+]. The first was an NM domain derived from the distantly related Candida albicans homolog of Sup35p (Sup35 NM<sub>CA</sub>-His<sub>7</sub>). As with S. cerevisiae Sup35p, the C. albicans protein supports prion-based inheritance in vivo and forms self-propagating amyloids in vitro. A species barrier, however, inhibits cross seeding between the S. cerevisiae and C. albicans proteins (14). A similar species barrier appears to exist in the liposome transformation, because we obtained only two [PSI+] colonies from 2846

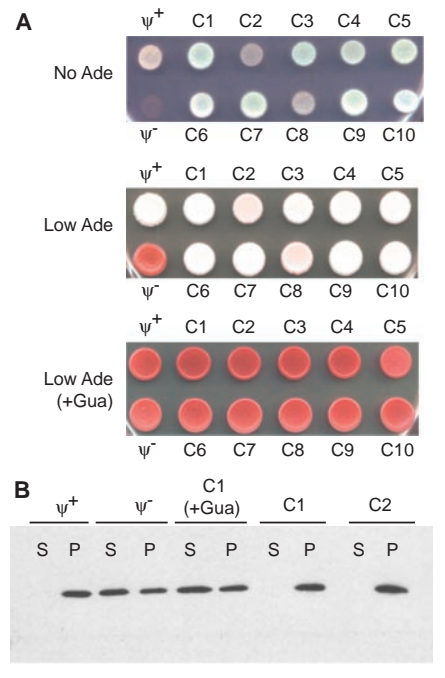


Fig. 4. Characterization of yeast converted by introduction of Sup35 NM-His, (A) Nonsense suppression phenotype of converted cells. The ability to suppress an ade1 nonsense mutation was examined by growth on medium lacking adenine, or containing low adenine with or without 5 mM guanidine (+Gua) as indicated. Shown are 10 examples of liposome-converted yeast (C1 to C10), as well as examples of  $[psi^-]$ and [PSI+] colonies. (B) For centrifugation assay examining solubility of Sup35p protein, cells were grown to mid-log phase, and extracts were subjected to centrifugation at 100,000g (9). Soluble (S) or pelleted (P) fractions were assayed by SDS-PAGE and Western blot analysis with a polyclonal antibody to Sup35p. Shown are two examples of liposome convertants (C1 and C2), a liposome convertant cured by growth on 5 mM guanidine (C1 + Gua), as well as  $[psi^-]$  and  $[PSI^+]$  strains.

transformants with liposomes containing the Sup35 NM<sub>CA</sub>-His<sub>7</sub> protein at a concentration of 200 µg/ml (Table 1).

The second Sup35p variant we examined was a single point mutant (substitution of serine at position 17 with arginine) of the S. cerevisae protein, which was identified in an earlier screen for Sup35p mutants that are defective in formation and propagation of the  $[PSI^+]$  prion state (19). Remarkably, this mutation, while not preventing prion formation, is sufficient to inhibit crossreaction with the wild-type protein in vivo and in vitro: The Sup35 NM fragment derived from this point mutant [Sup35 NM(S17R)-His<sub>7</sub>] forms amyloids fibers in vitro that are capable of seeding themselves but not the wild-type protein (Fig. 5A) (19). Similarly, whereas overexpression of the Sup35 NM-green fluorescent protein (GFP) fusion leads to ~30,000-fold increase in the rate of appearance of  $[PSI^+]$ , even prolonged massive overexpression of the mutant protein did not appreciably induce  $[PSI^+]$  (Fig. 5, B and C). This point mutation also abrogates the ability of the Sup35p to induce conversion by liposome transformants, because we obtained only a single [PSI<sup>+</sup>] colony out of 3852 liposomes transformation when liposomes contained Sup35 NM(S17R)-His, at a concentration of 200 µg/ml (Table 1).

Taken together, these results demonstrate the existence of a species barrier in the liposome transformations. In addition, because the production and purification of Sup35 NM(S17R)-His<sub>7</sub>, Sup35 NM<sub>CA</sub>-His<sub>7</sub> and wild-type Sup35 NM-His<sub>7</sub> are identical, the inability of the mutant proteins to induce [*PSI*<sup>+</sup>] argues strongly against the possibility that the observed infection is due to an undetected contaminant in our protein preparations.

**Table 1.** Effect of transfecting protein on the rates of  $[PSI^+]$  conversion. NM, NM<sub>CA</sub>, and NM(S17R) refer to Sup35 NM-His<sub>7</sub>, Sup35 NM<sub>CA</sub>-His<sub>7</sub>, and Sup35 NM(S17R)-His<sub>7</sub>, respectively. Unless otherwise indicated, protein concentrations were 200 μg/ml.

Transforming protein	[PSI+] convertants/ No. of transformants	Conver- sion rate (×10,000)
NM		
100 μg/ml	2/528	38
200 μg/ml	33/2,218	150
300 μg/ml	5/287	170
No	namyloid controls	
No protein	1/5,692	1.8
BSA	0/2,214	0
Si	pecificity controls	
NM <sub>CA</sub>	2/2,816	7.1
NM(S17R)	1/3,852	2.6
. ,	Total controls	
	4/14,574	2.7

In vitro-converted protein is far more efficient at inducing [PSI+] than protein produced by translation in vivo. Overexpression of Sup35p induces [PSI+] (Fig. 5, B and C) (12, 30). Thus, it was possible that the de novo conversion observed in our liposome transformation experiments was due to increasing the cellular levels of Sup35p over a critical threshold, rather than a consequence of the altered conformation of the introduced Sup35p. However, an average liposome delivers only 2 to 10% of the levels of endogenous protein (Fig. 2C) (25). Moreover, it is unlikely that yeast transformants receive substantially more Sup35-NM-His<sub>7</sub>, because increasing the level of protein in the liposomes to 300 to 500 µg/ml inhibits transformation. Thus, delivery of even substoichiometric quantities of preconverted protein by liposome fusion was sufficient to enhance greatly the rate of conversion to [PSI<sup>+</sup>]. By contrast, we found that transient expression of the identical Sup35 NM-Hispolypeptide to levels comparable to that of the endogenous protein had little effect on the rate of appearance of the  $[PSI^+]$  factor (26). Indeed, only after prolonged and massive overexpression of Sup35p NM domain (in this case fused to GFP) were we able to achieve efficiency of conversion comparable to that obtained by introduction of preconverted protein (Fig. 5C).

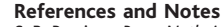
These results argue that infectivity is determined primarily not by the amount of protein exposed to the cytoplasm, but rather by the state of Sup35p. However, it remains unclear why the absolute numbers of conversion for both overexpression and liposome infection are in the range of only 1 to 3%. At

present, we cannot distinguish whether this is due to physiological factors, which make only a small fraction of yeast cells competent for conversion, or due to the quality of our encapsulated seed.

Conformation-based infectivity. Our studies provide direct evidence for the prion hypothesis: namely, that a protein, by virtue of its ability to propagate in an altered conformation, can act as an infectious agent. Using a liposome transformation protocol, we demonstrate that introduction of preconverted Sup35p-derived NM-His, protein into yeast cytoplasm can catalyze the aggregation of the cellular pool of Sup35p, resulting in de novo appearance of the well-characterized epigenetic factor [PSI+]. After induction, the [PSI<sup>+</sup>] state propagates indefinitely but is readily cured, without altering the cellular DNA, by transient growth on guanidine-containing medium.

Several observations argue that the ability of the introduced protein to convert yeast to [PSI<sup>+</sup>] is based on the protein's having adopted an altered, self-propagating conformation. First, mass spectroscopy reveals that the polypeptide contains no detectable covalent modifications. Second, in vitro seeding experiments demonstrate that before introduction into the yeast cytoplasm, the liposome-encapsulated protein has adopted the prion conformation capable of catalyzing the conversion of monomeric Sup35p. Third, conversion to  $[PSI^+]$  is induced only when the introduced seed is competent for seeding wild-type Sup35. Finally, the introduced, preconverted protein is vastly more effective at inducing the  $[PSI^+]$  state than is the identical polypeptide produced by translation in vivo.

The dramatic increase in infectivity of in vitro-converted Sup35 NM-His, compared with overexpression argues that, in vivo, there are specific and robust mechanisms for inhibiting de novo conversion of newly synthesized polypeptides. In part, this is accomplished by proteins, such as Sup45p, that specifically interact with Sup35p (31). However, recent observations suggest that the general cellular chaperone machinery also regulates prion formation and propagation (27, 32, 33). Recent analysis of sequenced genomes indicates that rather than being confined to a few proteins in yeast, glutamine and asparagine-rich domains with a high propensity to form selfpropagating prion states are present in a substantial fraction (~1%) of proteins in yeast and higher eukaryotes including mammals (34). Thus, in addition to promoting folding, the chaperone machinery is likely to help inhibit aggregation of cellular proteins with high glutamine and/or asparagine content into prionlike states. Once formed, however, chaperones appear to be unable to readily reverse polymerization of such highly ordered aggregates.



- S. B. Prusiner, Proc. Natl. Acad. Sci. U.S.A. 95, 13363 (1998).
- P. T. Lansbury, Proc. Natl. Acad. Sci. U.S.A. 96, 3342 (1999).
- D. L. Price, R. E. Tanzi, D. R. Borchelt, S. S. Sisodia, Annu. Rev. Genet. 32, 461 (1998).
- C. W. Olano and W. G. Tatton, Annu. Rev. Neurosci. 22, 123 (1999).
- G. P. Bates, L. Mangiarini, E. E. Wanker, S. W. Davies, Biochem. Soc. Trans. 26, 471 (1998).
- 6. R. B. Wickner, *Science* **264**, 566 (1994).
- T. R. Serio and S. L. Lindquist, Annu. Rev. Cell. Dev. Biol. 15, 661 (1999).
- 8. I. Stansfield et al., EMBO J. 14, 4365 (1995).
- B. S. Cox, M. F. Tuite, C. S. McLaughlin, Yeast 4, 159 (1988).
- M. D. Ter-Avanesyan et al., Mol. Microbiol. 7, 683 (1993).
- S. V. Paushkin, V. V. Kushnirov, V. N. Smirnov, M. D. Ter-Avanesyan, EMBO J. 15, 3127 (1996).
- M. M. Patino, J.-J. Liu, J. R. Glover, S. Lindquist, Science 273, 622 (1996).
- 13. L. Li and S. Lindquist, Science 287, 661 (2000).
- A. Santoso, P. Chien, L. Z. Osherovich, J. S. Weissman, Cell 100, 277 (2000).
- V. V. Kushnirov, N. V. Kochneva-Perukhova, M. B. Chechenova, N. S. Frolova, M. D. Ter-Avanesyan, EMBO J. 19, 324 (2000).
- Y. O. Chernoff et al., Mol. Microbiol. 35, 865 (2000).
   C. Y. King et al., Proc. Natl. Acad. Sci. U.S.A. 94, 6618 (1997).
- 18. j. R. Glover et al., Cell 89, 811 (1997).
- A. H. DePace, A. Santoso, P. Hillner, J. S. Weissman, Cell 93, 1241 (1998).
- 20. G. S. Jackson et al., Science 283, 1935, (1999).
- 21. K. Kaneko *et al.*, *J. Mol. Biol.* **295**, 997 (2000).
- 22. R. A. Bessen *et al.*, *J. Mot. Biol.* **293**, 997 (2000)
- D. C. Bolton, R. D. Rudelli, J. R. Currie, P. E. Bendheim, J. Gen. Virol. 72, 2905 (1991).
- 24. Supplemental Web material is available at *Science* Online at www.sciencemag.org/feature/data/1050406.shl.
- 25. At a concentration of 200 μg/ml, a 400-nm liposome contains ~200 molecules of Sup35p. By comparison, the endogenous concentration of

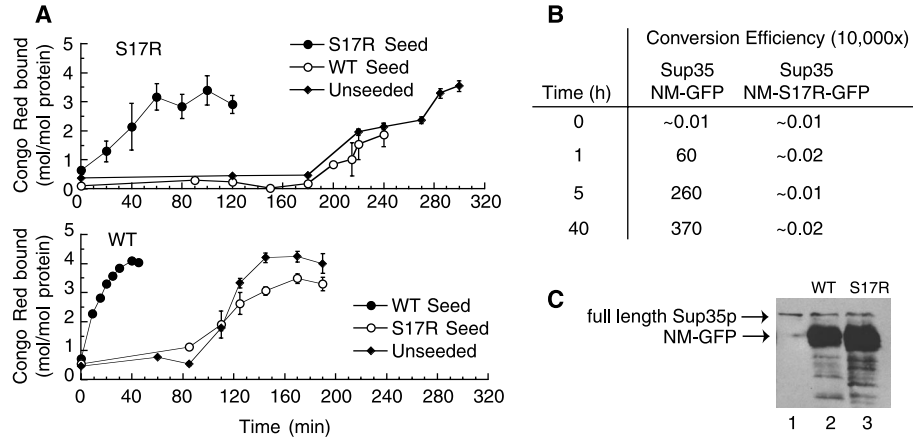


**Fig. 5.** Sup35 NM(S17R)-His $_7$  does not induce conversion of wild-type Sup35p in vitro or in vivo. (A) Wild-type and mutant Sup35p do not cross seed in vitro. Kinetics of conversion of Sup35 NM-His $_7$  (WT) or Sup35 NM(S17R)-His $_7$  was monitored as described in Fig. 3. Polymerization was followed either in the absence of seed or in the presence of 3% mol/mol ratio of preconverted wild-type or S17R mutant Sup35 NM-His $_7$  as indicated. Polymerization is enhanced only when the seed is the same as the converting protein. (B) Overexpression of mutant Sup35p fails to induce conversion to  $[PSI^+]$  in vivo. A fusion between GFP and either wild-type Sup35 NM or Sup35 NM(S17R) was expressed from a copper-inducible high-copy (2 $\mu$ ) plasmid (19). At the indicated times, the fraction of cells converted to  $[PSI^+]$  was determined by plating on medium lacking adenine. (C) Western blot analysis with an antibody raised against the Sup35 NM domain demonstrates that the wild-type (lane 2) and mutant (lane 3) proteins are expressed to comparable levels and are both strongly overexpressed relative to the endogenous full-length Sup35p (lane 1).

- Sup35p is at least 20-fold less than that of ribosomes, which are present at ~200,000 copies per yeast cell. See (35) for an estimate of ribosomes per yeast cell and (36, 37) for a quantification of Sup35p relative to ribosomes.
- H. E. Sparrer, A. Santoso, F. C. Szoka Jr., J. S. Weissman, unpublished data.
- Y. O. Chernoff, S. L. Lindquist, B.-i. Ono, S. G. Inge-Vechtomov, S. W. Liebman, *Science* 268, 880 (1995).
- 28. M. F. Tuite, C. R. Mundy, B. S. Cox, *Genetics* **98**, 691 (1981).
- 29. In preliminary experiments, we addressed the role of the [pin] element in yeast, which is an epigenetic modifier, that facilitates the formation of [PSI+] (38). We found that a stable [PSI+] state could also be introduced into an otherwise isogenic [pin-] strain of 74D-694, but the rate of conversion decreased substantially in the absence of [PIN+] factor. This is
- consistent with the proposal that the  $[PSI^+]$  phenotype can be induced and propagated independently of  $[PIN^+]$ , but that  $[PIN^+]$  facilitates  $[PSI^+]$  formation (39).
- Y. O. Chernoff, I. L. Derkach, S. G. Inge-Vechtomov, *Curr. Genet.* 24, 268 (1993).
- I. L. Derkatch, M. E. Bradley, S. W. Liebman, *Proc. Natl. Acad. Sci. U.S.A.* 95, 2400 (1998).
- G. P. Newnam, D. R. Wegrzyn, S. L. Lindquist, Y. O. Chernoff, *Mol. Cell. Biol.* 19, 1325 (1999); S. Krobitsch, S. L. Lindquist, *Proc. Natl. Acad. Sci. U.S.A.* 97, 1589 (2000).
- Y. O. Chernoff, G. P. Newnam, J. Kumar, K. Allen, A. D. Zink, Mol. Cell. Biol. 19, 8103 (1999).
- 34. M. D. Michelitsch and J. S. Weissman, in preparation.
- 35. J. R. Warner, *Trends Biochem. Sci.* **24**, 437 (1999)
- S. A. Didichenko, M. D. Ter-Avanesyan, V. N. Smirnov, Eur. J. Biochem. 198, 705 (1991).

- I. Stansfield, C. M. Grant, Akhmaloka, M. F. Tuite, Mol. Microbiol. 6, 3469 (1992).
- I. L. Derkatch, M. E. Bradley, P. Zhou, Y. O. Chernoff.
   W. Liebman, Genetics 147, 507 (1997).
- 39. I. L. Derkatch et al., EMBO J. 19,1942 (2000).
- 40. F. Szoka Jr. et al., Proc. Natl. Acad. Sci. U.S.A. 78, 1685 (1981).
- 41. We thank L. Gagne and M. Springer for assistance in liposome preparation and microscopy and F. E. Cohen, P. S. Kim, E. O'Shea, and members of the Lim and Weissman lab for helpful discussions. Supported by the NIH, the Searle Scholars Program, the David and Lucile Packard Foundation, and a postdoctoral fellowship from the European Molecular Biology Organization (H.E.S.).

15 March 2000; accepted 9 June 2000

## An Organic Solid State Injection Laser

J. H. Schön, Ch. Kloc, A. Dodabalapur, B. Batlogg\*

We report on electrically driven amplified spontaneous emission and lasing in tetracene single crystals using field-effect electrodes for efficient electron and hole injection. For laser action, feedback is provided by reflections at the cleaved edges of the crystal resulting in a Fabry-Perot resonator. Increasing the injected current density above a certain threshold value results in the decreasing of the spectral width of the emission from 120 millielectron volts to less than 1 millielectron volt because of gain narrowing and eventually laser action. High electron and hole mobilities as well as balanced charge carrier injection lead to improved exciton generation in these gate-controlled devices. Moreover, the effect of charge-induced absorption is substantially reduced in high-quality single crystals compared with amorphous organic materials.

Semiconductor lasers are widely used in modern science and technology. Compared with conventional inorganic semiconductors, organic semiconductors offer potential advantages with respect to easy processing, lower cost, and flexibility. Hence, electrically driven lasers based on organic semiconductors might find a wide range of applications. Optically excited lasing and amplified spontaneous emission have been observed in a wide range of semiconducting polymers, small molecules, and organic single crystals (1–9). Moreover, amorphous or nearly amorphous organic and polymeric semiconductors have been very successfully used in thin-film organic light-emitting devices (OLEDs). These devices typically require injection current densities of 1 to 10 mA/ cm<sup>2</sup> to achieve brightnesses of order 100 cd/m<sup>2</sup> (4). For laser applications, substantially higher current densities will be required. Reduced luminescence efficiencies at high injection current densities and charge-induced absorption have been identified as major problems for electrically pumped OLEDs (4, 10, 11). Another limiting factor is the low charge carrier mo-

Bell Laboratories, Lucent Technologies, 600 Mountain Avenue, Murray Hill, NJ 07974–0636, USA.

\*To whom correspondence should be addressed. E-mail: batlogg@lucent.com

bility. As an electrically driven device is strongly influenced by the transport properties of the semiconductor, we focus on organic materials that exhibit high mobilities for electrons as well as holes.

Materials properties. Mobilities on the order of 2 cm<sup>2</sup> V<sup>-1</sup> s<sup>-1</sup> can be achieved in tetracene at room temperature. This is more than four orders of magnitude higher than mobilities in materials used in conventional OLEDs (4, 8, 10). Tetracene also offers a reasonably high photoluminescence quantum yield, and electroluminescence has been reported for single-crystal diodes (12). Optically pumped amplified spontaneous emission has been observed in tetracene-doped (13, 14) and undoped anthracene single crystals (15). To minimize extrinsic influences such as grain boundaries, defects, or disorder, we investigated high-quality single crystalline samples to unveil the intrinsic opto-electronic properties of this material.

Device design. To ensure facile electrical contacts and balanced injection of electrons and holes, we used two field-effect electrodes. Tetracene single crystals were grown from the vapor phase in a stream of inert gas (16). Typical samples exhibit smooth faces of some mm<sup>2</sup> and thicknesses in the range of about 1 to 10 μm. Field-effect device struc-

tures were prepared on freshly cleaved crystal surfaces. Source and drain electrodes (Au for holes and Al for electrons, respectively) were thermally evaporated through a shadow mask defining a 25- $\mu$ m channel length and several hundred  $\mu$ m channel width. An amorphous Al<sub>2</sub>O<sub>3</sub> layer was sputtered onto the crystal, resulting in a capacitance of  $C_i = 50 \text{ nF/cm}^2$  between the gate electrode and the crystal. Finally, transparent Al-doped ZnO gate electrodes were deposited. A schematic of the structure is shown in Fig. 1A.

It has been recently demonstrated that ambipolar charge transport, i.e., n- as well as pchannel activity, can be obtained in high-quality single-crystal polyacene field-effect transistors (FETs) (17). Hence, gate-controlled electrodes can realize efficient electron as well as hole injection, with the field-induced charge acting as a heavily doped "contact" to the crystal. Furthermore, charge carrier mobilities as high as  $10^3$  to  $10^5$  cm<sup>2</sup> V<sup>-1</sup> s<sup>-1</sup> are achieved at low temperatures, and Fractional Quantum Hall transport has been observed in similar devices at temperatures below 4 K (18). Typical threshold voltages  $V_{\rm t}$  of the FETs are  $-0.6~{\rm V}$  for p-channel and +1 V for n-channel operation. The carrier concentration in the channel region can be adjusted by the applied gate voltage. Organic semiconductor crystals can act as a waveguide, as has been shown for optically pumped oligothiophene crystals (19, 20). However, in the present structure, the Al<sub>2</sub>O<sub>3</sub> layer  $(\sim 150 \text{ nm})$  is too thin to serve as a cladding layer. Thus, a planar multimode waveguide is formed by the entire structure with air as the cladding material on both sides. This means that at low injection current densities, a substantial fraction of the guided modes are in the lossy ZnO layers. The geometry of the device is such that there are many modes, and an analysis of the optics of this structure will be published elsewhere. An overall internal loss on the order of 100 cm<sup>-1</sup> is estimated for this multilayer structure. Feedback is provided by cleaving the crystal perpendicular to the waveguide structure, resulting in a Fabry-Perot-type resonator. Assuming an ideal reflectivity of 8% for these cleaved edges, mirror losses on the order of 50